Oxidative Addition of Palladium(0) Complexes Generated from [Pd(dba)$_2$] and P – N Ligands: A Kinetic Investigation**

Christian Amatore,* Alain Fuxa, and Anny Jutand*[a]

Dedicated to Professor Pierre Sinaÿ

Abstract: The major complex formed in solution from {[Pd^0(dba)$_2$] + 1 P – N} mixtures is [Pd^0(dba)(P – N)] (dba = *trans,trans*-dibenzylideneacetone; P – N = PhPN, 1-dimethylamino-2-diphenylphosphinobenzene; FcPN, *N,N*-dimethyl-1-[2-(diphenylphosphino)ferrocenyl]-methylamine; OxaPN, 4,4′-dimethyl-2-(2-diphenylphosphinophenyl)-1,3-oxazoline). Each complex consists of a mixture of isomers involved in equilibria: two 16-electron rotamer complexes [Pd^0(η^2-dba)(η^2-P – N)] and one 14-electron complex [Pd^0(η^2-dba)(η^1-P – N)] observed for FcPN and OxaPN. [Pd^0(dba)(PhPN)] and [*S*Pd^0(PhPN)] (*S* = solvent) react with PhI in an oxidative addition; [*S*Pd^0(PhPN)] is intrinsically more reactive than [Pd^0(dba)-(PhPN)]. This behavior is similar to that of the bidentate bis-phosphane ligands. When the PhPN ligand is present in excess, it behaves as a monodentate phosphane ligand, since [Pd^0(η^2-dba)(η^1-PhPN)$_2$] is formed first by preferential cleavage of the Pd–N bond instead of the Pd–olefin bond. [Pd^0(η^1-PhPN)$_3$] is also eventually formed. [Pd^0(dba)(FcPN)] and [Pd^0(dba)(Oxa-PN)] are formed whatever the excess of ligand used. [*S*Pd^0(FcPN)] and [*S*Pd^0(OxaPN)] are not involved in the oxidative addition. The 16-electron complexes [Pd^0(η^2-dba)(η^2-FcPN)] and [Pd^0(η^2-dba)(η^2-OxaPN)] are found to react with PhI via a 14-electron complex as has been established for [Pd^0(η^2-dba)(η^1-OxaPN)]. Once again, the cleavage of the Pd–N bond is favored over that of Pd–olefin bond. This work demonstrates the higher affinity for [Pd^0(P – N)] of dba compared with the P – N ligand, and emphasizes once more the important role of dba, which either controls the concentration of the most reactive complex, [*S*Pd^0(PhPN)], or is present in the reactive complexes, [Pd^0(dba)(FcPN)] or [Pd^0(dba)-(OxaPN)], and thus contributes to their intrinsic reactivity.

Keywords: kinetics · oxidative addition · palladium · P,N ligands

Introduction

[Pd^0(dba)$_2$] (dba = *trans,trans*-dibenzylideneacetone) together with phosphane ligands is frequently used as a source of palladium(0) complexes in catalytic reactions. We have established that the dba ligand plays a crucial role in both the structure and the reactivity of the palladium(0) complexes generated in situ from [Pd^0(dba)$_2$] and phosphane ligands.[1] Whatever the monodentate phosphane[1, 2] ligand L under investigation, two main complexes, [Pd^0(dba)L$_2$] and [*S*Pd^{0}L$_3$] (*S* = solvent), are formed from {[Pd^0(dba)$_2$] + *n* L} when $n \geq 3$.[3] The major complex is [Pd(dba)L$_2$], but the most reactive species in the oxidative addition to phenyl iodide is the lowest ligated complex [*S*PdL$_2$], which is involved in two equilibria with [Pd^0(dba)L$_2$] and [*S*Pd^{0}L$_3$] (Scheme 1).

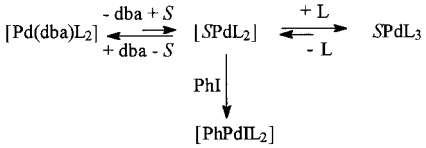

Scheme 1. Equilibria involving the complex [*S*PdL$_2$].

Whatever the nature of the bidentate phosphane ligand L – L under investigation (1,2-bis(diphenylphosphino)ethane (dppe), 1,3-bis(diphenylphosphino)propane (dppp), 4,5-bis-(diphenylphosphinomethyl)-2,2-dimethyl-2,2-dimethyl-1,3-dioxolane (diop), 1,1′-bis(diphenylphosphino)ferrocene (dppf), [1,1′-binaphthalene]-2,2′-diylbis(diphenylphosphine) (binap)), the major complex formed from {[Pd^0(dba)$_2$] + *n* L – L} when $n = 1$ is [Pd(dba)(L – L)], but the most reactive species in the oxidative addition is again the low-ligated complex [*S*PdL$_2$] which is involved in an endergonic equilibrium with [Pd^0(dba)(L – L)] (Scheme 2).[1, 4] However, in

[a] Dr. C. Amatore, Dr. A. Jutand, Dr. A. Fuxa
Ecole Normale Supérieure, Département de Chimie
UMR CNRS 8640, 24 Rue Lhomond, 75231 Paris Cedex 5 (France)
Fax: (+33) 144-323-863
E-mail: Amatore@ens.fr
Anny.Jutand@ens.fr

[**] dba = trans,trans-dibenzylideneacetone; P – N = 1-dimethylamino-2-diphenylphosphinobenzene; *N,N*-dimethyl-1-[2-(diphenylphosphino)ferrocenyl]methylamine; 4,4′-dimethyl-2-(2-diphenylphosphinophenyl)-1,3-oxazoline.

0947-6539/00/0608-1474 $ 17.50+.50/0 *Chem. Eur. J.* **2000**, *6*, No. 8

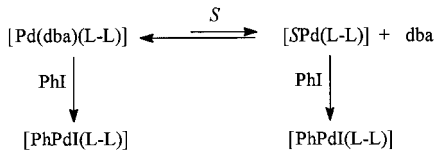

Scheme 2. Reaction of [Pd(dba)(L–L)] with PhI.

contrast to the monophosphanes, [Pd(dba)(L–L)] also reacts with phenyl iodide. When $n \geq 2$, the unreactive [Pd(L–L)$_2$] complex is formed (except for with binap).[4]

The overall reactivity is jointly governed by the intrinsic reactivity of [*S*PdL$_2$] or [*S*Pd(L–L)] in the oxidative addition step and by their concentration, which is controlled by equilibria involving dba. This is why dba plays such a crucial role by tuning the concentration of the most reactive Pd^0 complex.

P–N ligands are considered as bidentate ligands. The phosphorus atom coordinates the palladium(0) center more strongly than does the nitrogen atom. Such P–N ligands may thus behave as either bidentate or monodentate ligands (Scheme 3 in which the other ligands of Pd^0 are omitted) with

Scheme 3. Bi- or monodentate nature of the P–N ligand.

kinetic and structural consequences since they may contribute to the enantioselectivity observed in organic reactions catalyzed by palladium ligated to chiral P–N ligands.[5–10]

We report here our results on the characterization of palladium(0) complexes generated from [Pd(dba)$_2$] and P–N ligands, and also their reactivity in oxidative addition. Phenyl iodide was chosen as a model compound for the oxidative addition to allow comparison with our previous work. Three ligands were selected for study: PhPN, FcPN, and OxaPN.

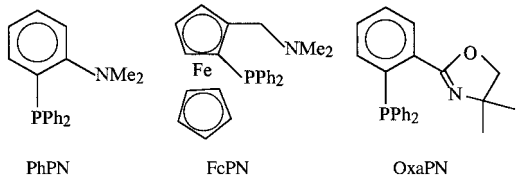

PhPN FcPN OxaPN

FcPN and OxaPN are models for the aminoferrocenylphosphane[11] and phosphinooxazoline[12] ligands, respectively, that are used in enantioselective cross-coupling reactions,[5] allylic nucleophilic substitutions,[6–8] and Heck reactions.[9] Both of these ligands form six-membered-ring palladium(0) complexes. PhPN[13] was selected because of its more rigid structure which leads to five-membered-ring palladium(0) complexes.

Abstract in French: *Les complexes [Pd^0(dba)(P–N)] (P–N = PhPN, 1-diméthylamino-2-diphénylphosphinobenzène; FcPN, N,N-diméthyl-1-[2-(diphénylphosphino)ferrocényl]méthylamine; OxaPN, 4,4′-diméthyl-2-(2-diphényl-phosphinophényl)-1,3-oxazoline) sont les complexes majoritaires formés en solution à partir de {[Pd^0(dba)$_2$] + 1 P–N}. Il se forme plusieurs complexes isomères en équilibre: deux rotamères [Pd^0(η^2-dba)(η^2-P–N)] (complexes à 16 électrons) et un complexe à 14 électrons, [Pd^0(η^2-dba)(η^1-P–N)] seulement observé pour les ligands FcPN et OxaPN. [Pd^0(dba)(PhPN)] et [SPd^0(PhPN)] réagissent avec PhI dans une réaction d'addition oxydante, [SPd^0(PhPN)] est intrinsèquement plus réactif que [Pd^0(dba)(PhPN)]. Ce comportement est similaire à celui déjà décrit pour les ligands bisphosphanes. Quand le ligand PhPN ligand est en large excès, il se comporte comme un ligand phosphane monodentée puisque [Pd^0(η^2-dba)(η^1-PhPN)$_2$] est d'abord formé par suite de la rupture préférentielle de la liaison Pd–N, le palladium(0) restant lié à la double liaison du ligand dba. [Pd^0(η^1-PhPN)$_3$] est ensuite formé. [Pd^0(dba)(FcPN)] et [Pd^0(dba)(OxaPN)] se forment quel que soit l'excès de ligand. [SPd^0(FcPN)] et [SPd^0(OxaPN)] ne sont pas impliqués dans la réaction d'addition oxydante. Les complexes à 16 électrons, [Pd^0(η^2-dba)(η^2-FcPN)] et [Pd^0(η^2-dba)(η^2-OxaPN)] réagissent avec PhI via les complexes à 14 électrons comme cela a été établi pour [Pd^0(η^2-dba)(η^1-OxaPN)]. Une fois de plus, la rupture de la liaison Pd–N est plus facile que celle de la liaison Pd–oléfine. Ces résultats mettent en évidence une plus grande affinité du ligand dba pour [Pd^0(P–N)] que celle du ligand P–N et confirment une fois de plus le rôle important du ligand dba qui soit contrôle la concentration du complexe le plus réactif, [SPd^0(PhPN)], ou est présent dans les complexes réactifs, [Pd^0(dba)(FcPN)] et [Pd^0(dba)(OxaPN)], et donc contribue à leur réactivité intrinsèque.*

Results and Discussion

Identification of the palladium(0) complexes generated from {[Pd(dba)$_2$] + *n* P–N} ($n \geq 1$) in THF

Cyclic voltammetry was used to determine the quantity of dba released when *n* equivalents of P–N were added to [Pd(dba)$_2$] in THF. This technique takes advantage of 1) the characteristic cyclic voltammogram of dba (it exhibits one reversible one-electron reduction peak R_1 at -1.27 V vs. SCE followed by a one-electron irreversible reduction peak R_2 at -1.90 V vs. SCE)[1] and 2) the fact that the reduction peak current at R_1 is proportional to the concentration of free dba. The palladium(0) complexes were also investigated by ^{31}P NMR and UV spectroscopy. As already reported, palladium(0) complexes ligated by two phosphane ligands and dba exhibit one absorption band at around 350–400 nm, which is characteristic of the ligated dba.[1, 14]

[Pd(dba)$_2$] + 1 P–N: With any of the P–N ligands (PhPN, FcPN, and OxaPN), [Pd(dba)(P–N)] complexes were formed after addition of one equivalent of the ligand to [Pd(dba)$_2$] in THF [Eq. (1)]. Indeed, one equivalent of free dba was

$$[Pd^0(dba)_2] + P\text{–}N \longrightarrow [Pd^0(dba)(P\text{–}N)] + dba \quad (1)$$

detected by cyclic voltammetry (Figure 1a), which proves that the resulting palladium(0) complex contains only one ligated dba. That the oxidation peak of $[Pd^0(dba)_2]$ at +1.26 V was no longer observed shows that a stoichiometric reaction took

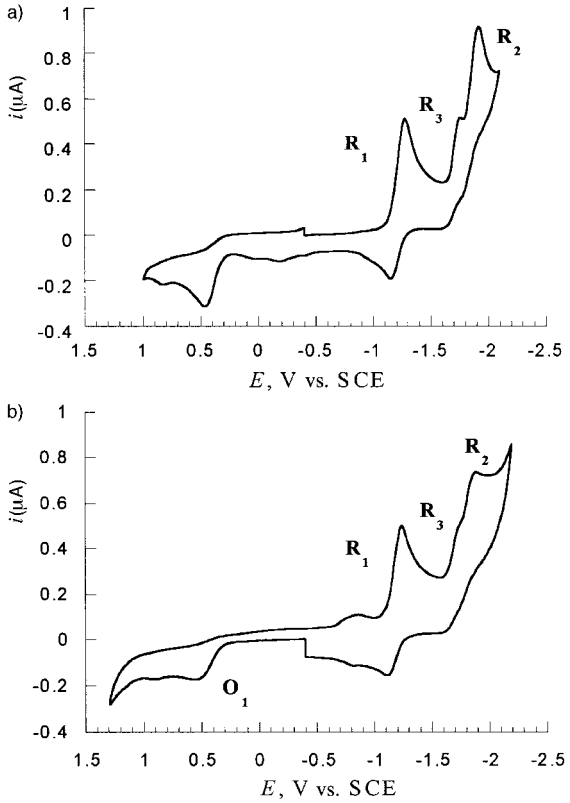

Figure 1. Cyclic voltammograms of a solution of $[Pd(dba)_2]$ (2 mmol dm^{-3}) and one equivalent of PhPN in THF (containing nBu$_4$NBF$_4$, 0.3 mmol dm^{-3}) at a stationary gold disk electrode (0.5 mm diameter) with a scan rate of 0.5 V s^{-1}. a) Reduction first. b) Oxidation first.

Table 1. Oxidation peak potential and UV spectroscopy of Pd^0 complexes generated from {$[Pd(dba)_2]$ + 1P–N} in THF.

P–N	$[Pd(\eta^2\text{-dba})(\eta^2\text{-P–N})]$	
	E^p_{Ox} [V][a]	UV [λ_{max} nm]
PhPN	+0.52	386
OxaPN	+0.47	387
FcPN	+0.50, +0.85[b]	387

[a] Potentials are relative to SCE electrode. They were determined in THF containing nBu$_4$NBF$_4$, 0.3 mol dm^{-3}, at a gold disk electrode (i. d. = 0.5 mm) with a scan rate of 0.5 V s^{-1} at 20 °C. [b] Reversible oxidation peak of the ferrocenyl ligand of the palladium(II) complex formed after oxidation of $[Pd^0(dba)(FcPN)]$.

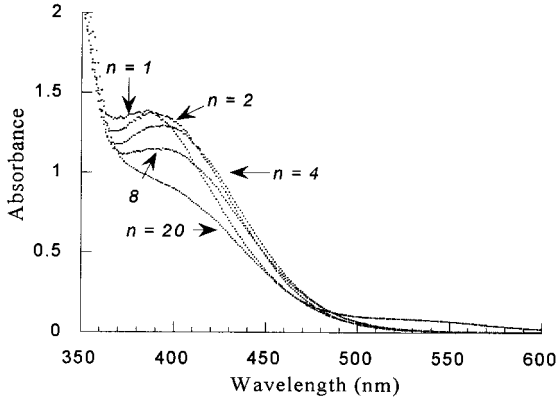

Figure 2. UV spectra of a solution of $[Pd(dba)_2]$ (1 mmol dm^{-3}) and n (n = 1, 2, 4, 8, 20) equivalents of PhPN in THF in a 1 mm path cell at 20 °C.

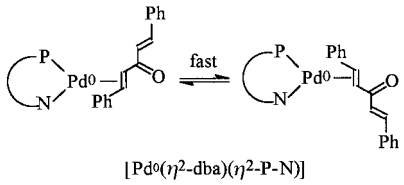

Scheme 4. Formation of $[Pd^0(\eta^2\text{-dba})(\eta^2\text{-P–N})]$.

place in which one Pd^0 center coordinates one P–N ligand [Eq. (1)]. Consequently the new oxidation peak present in the voltammogram (Figure 1b, Table 1) can safely be assigned to $[Pd^0(dba)(P–N)]$. The presence of one ligated dba was also confirmed by UV spectroscopy (Figure 2, Table 1).

Since dba usually participates in η^2 ligation in palladium(0) complexes,[1] two different 16-electron complexes Pd(η^2-dba)(η^2-P-N) may be formed (Scheme 4).[15] Similar complexes have been isolated and characterized in which the palladium(0) center is ligated by a P–N ligand and a symmetrical olefin such as dimethyl fumarate or maleic anhydride.[16]

$[Pd^0(dba)(PhPN)]$ formed in situ from {$[Pd(dba)_2]$ + 1 PhPN} exhibited a single ^{31}P NMR signal δ_1 at room temperature (Table 2), but this signal decoalesced with decreasing temperature. Two signals of different magnitude could then be observed at 260 K (Table 2) which were not affected by addition of dba. This indicates that two isomers of

Table 2. ^{31}P NMR chemical shifts of palladium(0) complexes generated from {$[Pd(dba)_2]$ + nP–N} (n = 1, 2) and of [PhPdI(P–N)] complexes formed in the oxidative addition with PhI in THF when n = 1.

	P–N δ_0[a]	$[Pd(\eta^2\text{-dba})(\eta^2\text{-P–N})]$ δ_1	$[Pd(\eta^2\text{-dba})(\eta^1\text{-P–N})]$ δ_2	$[Pd(\eta^2\text{-dba})(\eta^1\text{-P–N})_2]$ δ_3[a] δ_4[a]	[PhPdI(P–N)] δ_5[a]
PhPN	–12.10	16.21[a] 15.77,[c] 16.75[c]	n. o.[b]	20.11 (br d), 24.83 (br d)	25.30
OxaPN	–4.82	18.94 (br s 80%)[a] 17.33,[c] 20.02[c] (50%, 50%)	18.55 (s 20%)[a] 18.22 (s)[c]	n. o.[b]	19.95
FcPN	–22.82	11.63 (94%)[d] 10.88,[e] 11.57[e] (4%, 96%)	12.30 (6%)[d] 12.90[e]	n. o.[b]	15.96

[a] In ppm vs. H_3PO_4 at 293 K. [b] n. o.: not observed. [c] At 260 K. [d] At 280 K. [e] At 230 K.

0947-6539/00/0608-1476 $ 17.50+.50/0 Chem. Eur. J. 2000, 6, No. 8

[Pd(η^2-dba)(η^2-PhPN)] are formed as postulated in Scheme 4 and are involved in a fast equilibrium at room temperature. The ^{1}H NMR spectrum of free PhPN exhibited one unique singlet for the two methyl groups at $\delta = 2.44$. In [Pd^0(dba)(PhPN)], four singlets were observed at $\delta = 3.07$, 2.55, 2.31, and 2.15 that correspond to diastereotopic methyl groups. This is evidence for the ligation of the palladium(0) center by the nitrogen atoms of the P–N ligand in two different [Pd^0(η^2-dba)(η^2-PhPN)] isomers (as in Scheme 4) which are interconverted by a fast olefin rotation (Scheme 5).

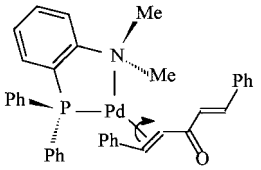

Scheme 5. Interconversion of the two [Pd^0(η^2-dba)(η^2-PhPN)] isomers by fast olefin rotation.

At 293 K, the ^{31}P NMR spectrum of [Pd^0(dba)(OxaPN)] exhibited two ^{31}P NMR signals δ_1 and δ_2 with different magnitudes thus demonstrating the existence of two different palladium(0) complexes (Table 2). At lower temperatures, the broad signal ($\Delta\nu_{1/2} = 52$ Hz) at $\delta_1 = 18.94$ split into two signals of almost equal magnitude (Table 2). Two isomeric complexes [Pd^0(η^2-dba)(η^2-OxaPN)] coexist, which are rapidly interconverted at room temperature (Scheme 4). The exchange rate constant k between the two [Pd^0(η^2-dba)(η^2-OxaPN)] isomers has been determined from ^{31}P NMR spectroscopy,[17] and the Arrhenius plot provides an activation energy of 51 kJ mol^{-1} (Figure 3). This relatively low value suggests that the fast isomerization of [Pd^0(η^2-dba)(η^2-OxaPN)] complexes observed at room temperature involves a fast intramolecular rotation of dba around the C=C bond.[16, 18] Decoordination–recoordination of dba is excluded because the isomerization process was not affected by the dba concentration.

The signal at $\delta_2 = 18.55$ (Table 2) did not decoalesce with decreasing temperature. Kinetic investigations into the oxidative addition reaction (vide infra) suggest that it belongs to the 14-electron complex [Pd^0(η^2-dba)(η^1-OxaPN)] (Scheme 6). Analogous complexes formed by Pd–N bond cleavage have been characterized in palladium(0) complexes ligated by a P–N ligand and a symmetrical olefin such dimethyl fumarate or maleic anhydride.[16a–b] As will be established later, this 14-electron complex is involved in an equilibrium with [Pd^0(η^2-dba)(η^2-OxaPN)] complexes at room temperature (Scheme 6).

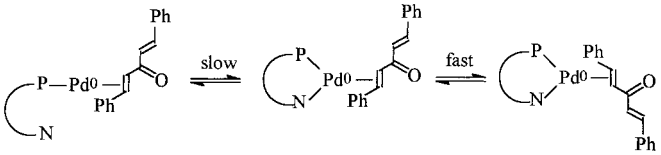

Scheme 6. Isomers involved in equilibria for [Pd^0(η^2-dba)(FcPN)] and [Pd^0(η^2-dba)(OxaPn)].

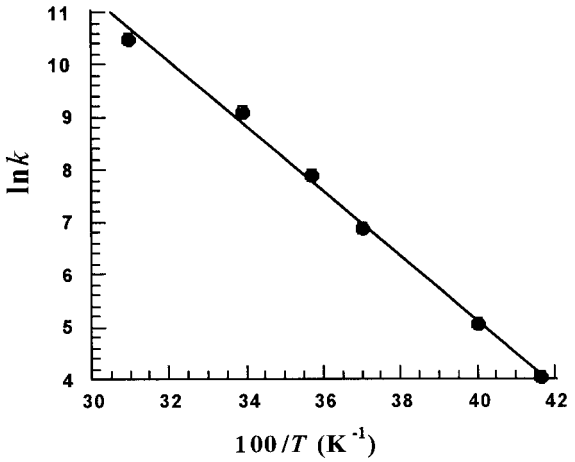

Figure 3. Arrhenius plot for the exchange reaction between the two isomers [Pd^0(η^2-dba)(η^2-OxaPN)] (Scheme 4) determined from ^{31}P NMR measurements (162 MHz) performed at various temperatures on a solution of [Pd(dba)$_2$] (14 mmol dm^{-3}) and OxaPN (1 equiv) in THF (3 mL) with [D$_6$]acetone (0.2 mL) (H_3PO_4 as external reference).

At 313 K, [Pd^0(η^2-dba)(FcPN)] displayed one ^{31}P NMR signal at $\delta = 11.82$, whereas at 280 K, two signals appeared at δ_1 and δ_2 (Table 2). At 230 K, the signal at δ_1 split into two signals (Table 2), while δ_2 remained unaltered. This indicates that three isomers are formed, two of them being involved in a fast equilibrium as for OxaPN (Scheme 6).

[Pd(dba)$_2$] + nP–N ($n \geq 2$): In [Pd^0(dba)(FcPN)] and [Pd^0(dba)(OxPN)], the dba ligand was displaced by an excess of P–N ligand [$n \geq 2$, Eq. (2)]. The ^{31}P NMR spectra

$$[Pd^0(dba)_2] + n\,P\text{–}N \longrightarrow [Pd^0(dba)(P\text{–}N)] + dba + (n-1)\,P\text{–}N \quad (n \geq 2) \qquad (2)$$

remained similar to those described above on addition of the P–N ligand (Table 2). The cyclic voltammograms also remained unaltered by addition of an excess of P–N ligand. Consequently, neither the 18-electron complexes [Pd^0(η^2-FcPN)$_2$] and [Pd^0(η^2-OxaPN)$_2$] nor the 16-electron complexes [Pd^0(η^2-FcPN)(η^1-FcPN)] and [Pd^0(η^2-OxPN)(η^1-OxaPN)] were formed, which demonstrates the higher affinity of the dba ligand for [Pd^0(P–N)] than that of the P–N ligand.

A more complex situation was encountered for the PhPN ligand. For $n = 2$, the δ_1 signal of [Pd^0(η^2-dba)(η^2-PhPN)] became broader and a group of two signals δ_3 and δ_4 of equal integration (Table 2) appeared as broad doublets, characterizing two different ^{31}P atoms on the same molecule. Some free PhPN ligand was observed as shown by the presence of its broad signal δ_0 (Table 2). Addition of four equivalents of PhPN per [Pd(dba)$_2$] resulted in the complete disappearance of [Pd^0(η^2-dba)(η^2-PhPN)]. Only the new complex (δ_3, δ_4) could be observed together with the free ligand. All this evidence suggests that a new complex with two nonequivalent

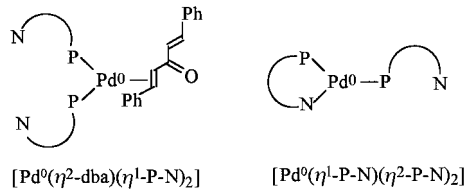

^{31}P atoms is formed with a large excess of PhPN, and that it is involved in an equilibrium with the P–N ligand and [Pd^0(η^2-dba)(η^2-PhPN)]. Two 16-electron complexes with two PhPN ligands with nonequivalent ^{31}P atoms may be formed: either [Pd(η^2-dba)(η^1-PhPN)$_2$] or [Pd(η^1-PhPN)(η^2-PhPN)].

Discrimination between the two structures was achieved with UV spectroscopy. The UV spectrum of {[Pd(dba)$_2$] + 4 PhPN} exhibited an absorption band at $\lambda_{max} = 393$ nm, which is slightly shifted to higher wavelengths than that of [Pd^0(η^2-dba)(η^2-PhPN)] ($\lambda_{max} = 387$ nm) (Figure 2). Moreover, since [Pd^0(η^2-dba)(η^2-PhPN)] was no longer visible in the ^{31}P NMR spectrum, this established that the new palladium(0) complex (which contains two different ^{31}P atoms) also contains one dba ligand[14] as in [Pd^0(η^2-dba)(η^1-PhPN)$_2$][19] and that PhPN (when $n \leq 4$) cannot displace dba from [Pd^0(η^2-dba)(η^2-PhPN)] [Eq. (3)]. Cleavage of the Pd–N bond is thus preferred to Pd–olefin bond cleavage.

$$[\underset{\delta_1}{Pd^0(\eta^2\text{-dba})(\eta^2\text{-PhPN})}] + \underset{\delta_0}{PhPN} \overset{K}{\rightleftharpoons} [\underset{\delta_3,\,\delta_4}{Pd^0(\eta^2\text{-dba})(\eta^1\text{-PhPN})_2}] \quad (3)$$

The ^{31}P NMR spectrum of the {[Pd(dba)$_2$] + 2 PhPN} mixture was not modified by addition of dba (10 equivalents), which indicates that dba is not involved in the equilibrium [Eq. (3)]. The equilibrium constant K was calculated from the magnitude of the ^{31}P NMR signals of the {[Pd(dba)$_2$] + 2 PhPN} mixture (Table 2) as in Equation (4), such that

$$K = \frac{[Pd^0(dba)(PhPN)_2]}{([Pd^0(dba)(PhPN)] \times [PhPN])} = \frac{(S_{\delta_0} + S_{\delta_3})}{(S_{\delta_3} \times C_0)} \quad (4)$$

$KC_0 = 1.4$ (± 0.1), where C_0 is the initial concentration of [Pd(dba)$_2$]. The absorbance of [Pd^0(η^2-dba)(η^1-PhPN)$_2$] at 393 nm quickly decreased and reached a constant value upon successive additions of an excess of PhPN ($n > 4$) (Figure 2). This shows that [Pd^0(η^2-dba)(η^1-PhPN)$_2$] is involved in an equilibrium with the ligand [Eq. (5); step a = Eq. (3)] and that

$$[Pd^0(\eta^2\text{-dba})(\eta^2\text{-PhPN})] \underset{\text{step a}}{\overset{+\text{PhPN}}{\underset{K}{\rightleftharpoons}}} [Pd^0(\eta^2\text{-dba})(\eta^1\text{-PhPN})_2] \underset{\text{step b}}{\overset{+\text{PhPN},\ -\text{dba}}{\underset{K'}{\rightleftharpoons}}} [Pd^0(\eta^1\text{-PhPN})_3] \quad (5)$$

dba is progressively released from [Pd^0(η^2-dba)(η^1-PhPN)$_2$] by incorporation of a third molecule of PhPN. This affords a 16-electron complex [Pd^0(η^1-PhPN)$_3$] in which PhPN acts as a monodentate ligand [Eq. (5)].

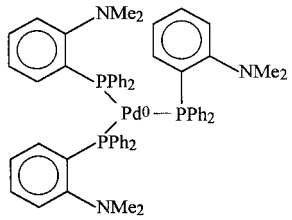

[Pd^0(η^1-PhPN)$_3$]

When four equivalents of PhPN were added to [Pd(dba)$_2$] (1 mmol dm^{-3}), the equilibrium of Equation (3) was totally shifted towards [Pd^0(η^2-dba)(η^1-PhPN)$_2$] since the ^{31}P NMR signal δ_1 of [Pd^0(η^2-dba)(η^2-PhPN)] was no longer visible. The decay of the absorption band of [Pd^0(η^2-dba)(η^1-PhPN)$_2$] at 393 nm, when more than four equivalents of PhPN were added, allowed an estimation of $K' \approx 2.7 \times 10^{-2}$ [Eq. (5)]. The low value of K' indicates that dba remains a better ligand for [Pd^0(η^1-PhPN)$_2$] than PhPN, so that a large amount of PhPN is required to displace the dba completely from [Pd^0(η^2-dba)(η^1-PhPN)$_2$] to generate [Pd^0(η^1-PhPN)$_3$] ($n \gg 20$).

Identification of the reactive palladium(0) complexes generated from {[Pd(dba)$_2$] + 1 P–N} in the oxidative addition to PhI

For every P–N ligand investigated here, the oxidative addition of PhI to palladium(0) complexes generated in situ from {[Pd(dba)$_2$] + 1 P–N} quantitatively afforded a single arylpalladium(II) complex characterized by its ^{31}P NMR signal [Table 2, Eq. (6)]. The same [PhPdI(P–N)] complexes were formed independently by substitution of PPh$_3$ by P–N ligands in *trans*-[PhPdI(PPh$_3$)$_2$] complexes [Eq. (7)] .

$$\{[Pd^0(dba)_2] + 1\,P\text{–}N\} + PhI \longrightarrow [PhPdI(P\text{–}N)] + 2\,dba \quad (6)$$

$$\textit{trans}\text{-}[PhPdI(PPh_3)_2] + P\text{–}N \longrightarrow [PhPdI(P\text{–}N)] + 2\,PPh_3 \quad (7)$$

The ^{31}P NMR signal of [PhPdI(P–N)] did not decoalesce with decreasing temperature, which suggests that only one isomer was formed and that the structure of the final arylpalladium(II) complex does not depend on the nature of the palladium(0) mixture that reacts in the oxidative addition.

With all the P–N ligands investigated here, all of the ^{31}P NMR signals for palladium(0) complexes disappeared in the presence of PhI. This indicates either that all the palladium(0) complexes react with PhI in parallel or that one complex is more reactive and pulls all the other palladium(0) complexes through the continuous displacement of the equilibria described above. The kinetics of the oxidative addition to PhI were investigated in THF at 40 °C by two different analytical techniques: either UV spectroscopy[14] by measuring the decay of the absorption band of [Pd^0(dba)(P–N)] versus time (Figure 4a) or steady amperometry[2] by recording the decay of the oxidation current of [Pd^0(dba)(P–N)] complexes versus time (Figure 4c). The plot of either $\ln[(D_0 - D_{inf})/(D - D_{inf})]$ or $\ln(i_0/i)$ versus time [Eq. (8)] afforded straight lines with similar slopes k_{app} (Figure 4b, 4d).

$$\ln\left(\frac{i_0}{i}\right) = \ln\left(\frac{D_0 - D_{inf}}{D - D_{inf}}\right) = \ln\left(\frac{[Pd^0]_0}{[Pd^0]}\right) = k_{app}t \quad (8)$$

Both methods afford similar results, but amperometry is more appropriate for fast reactions. In all cases [Pd^0(dba)(P–N)] was found to be the major complex in solution (see above). In order to identify the true reactive palladium(0) complex involved in the oxidative addition, the reaction order in PhI was determined by plotting the apparent rate constant k_{app} versus the PhI concentration (Figure 5a–c).

With the PhPN ligand the reaction order in PhI is not strictly one (Figure 5a) as had been established for the bidentate P–P ligand[4] (Scheme 2), $k_{app} = A + B[PhI]$. The rate of the oxidative addition was slower in the presence of

0947-6539/00/0608-1478 $ 17.50+.50/0 *Chem. Eur. J.* **2000**, *6*, No. 8

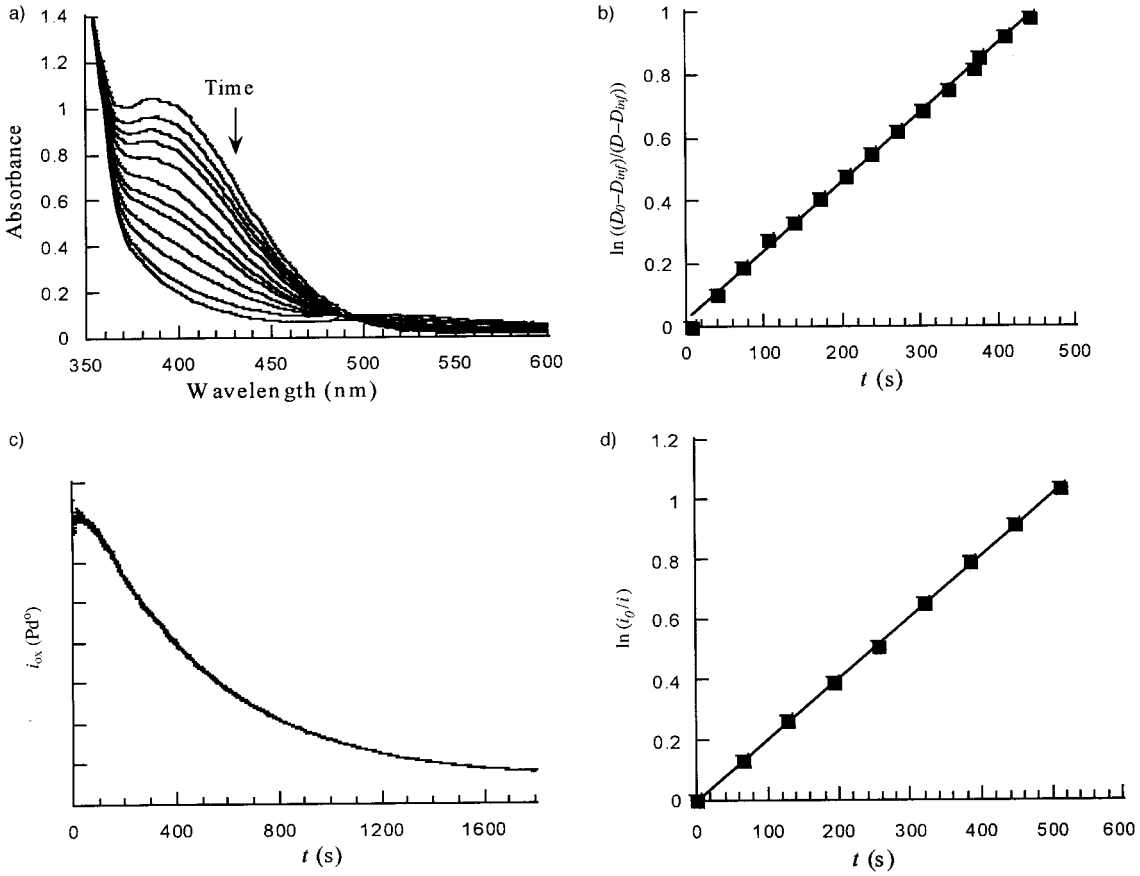

Figure 4. Oxidative addition of PhI to the palladium(0) complex generated in situ from a {[Pd(dba)$_2$] + 1 OxaPN} mixture in THF at 40 °C. a) and b) Kinetics monitored by UV spectroscopy of a solution of [Pd(dba)$_2$] (1 mmol dm^{-3}) and OxaPN (1 mmol dm^{-3}); a) UV spectrum of [Pd^0(dba)(OxaPN)] recorded versus time in the presence of PhI (0.3 mol dm^{-3}); b) plot of $\ln[(D_0 - D_{inf})/(D - D_{inf})] = \ln([Pd^0]_0/[Pd^0])$ versus time (D_0 = initial absorbance of [Pd^0(dba)(OxaPN)], D = absorbance of [Pd^0(dba)(OxaPN)] at t, D_{inf} = absorbance of [Pd^0(dba)(OxaPN)] at infinite time). c) and d) Kinetics monitored by amperometry at a rotating gold disk electrode (i. d. = 2 mm, $\omega = 105$ rad s^{-1}) with a solution of [Pd(dba)$_2$] (2 mmol dm^{-3}) and OxaPN (2 mmol dm^{-3}); c) variation of the oxidation current of [Pd^0(dba)(OxaPN)] at +0.6 V versus time in the presence of PhI (0.3 mol dm^{-3}); d) plot of $\ln(i_0/i) = \ln([Pd^0]_0/[Pd^0])$ versus time (i = oxidation current of [Pd^0(dba)(OxaPN)] at t, i_0 = initial oxidation current of [Pd^0(dba)(OxaPN)]).

dba (Figure 5a). This indicates that the more reactive species is [*S*Pd^0(PhPN)], which is involved in an equilibrium with [Pd^0(dba)(PhPN)] complexes and dba. However, the [Pd^0(dba)(PhPN)] complexes also react with PhI (Scheme 7). Equation (9) has been established for P–P ligands.[4]

$$k_{app} = k_0[PhI] + \frac{k_1 k_2[PhI]}{k_{-1}[dba] + k_2[PhI]} \quad (9)$$

One may assume that when the dba concentration is low (that is, when no excess of dba is present) $k_{-1}[dba] \ll k_2[PhI]$, so that Equation (9) simplifies to $k_{app} = k_1 + k_0[PhI]$, which is identical to the experimental equation (Figure 5a). The values of k_0 and k_1 are thus determined from the slope and intercept of this plot: $k_0 = 3.4 \times 10^{-2}$ mol^{-1} dm^3 s^{-1} and $k_1 = 1.3 \times 10^{-2}$ s^{-1}.

The 16-electron complex [Pd^0(η^2-dba)(η^2-PhPN)] is in fact a mixture of two isomers (Scheme 4) involved in a fast equilibrium at room temperature. From the kinetic data it is thus impossible to determine which is the reactive isomer.[20]

For the FcPN ligand, the reaction order in PhI is strictly one within experimental precision (Figure 5b) and $k_{app} = A[PhI]$. Moreover the rate of the oxidative addition was not affected when the dba concentration was increased, which is quite unusual for a monodentate or bidentate phosphane ligand.[1] This establishes that the reactive species is a [Pd^0(dba)(FcPN)] complex and not [*S*Pd^0(FcPN)] as usually observed (Scheme 8). These two complexes are probably involved in a very endergonic equilibrium so that the concentration of [Pd^0(FcPN)] is so low that it does not react appreciably with PhI in comparison with the direct reaction of [Pd^0(η^2-dba)(FcPN)].

Three [Pd^0(dba)(FcPN)] complexes are present: two rotamers [Pd^0(η^2-dba)(η^2-FcPN)] and [Pd^0(η^2-dba)(η^1-FcPN)] involved in equilibria (Scheme 6). The reaction order in PhI is one, which means that the equilibria that provide the reactive complex are always faster than the oxidative addition step. Consequently the more reactive species cannot be identified from kinetic investigations even if the 14-electron complex [Pd^0(η^2-dba)(η^1-FcPN)] is probably the most reactive complex (although less electron rich, it is less hindered for the PhI approach). The rate constant k_0 of the overall reaction (Scheme 8) was nevertheless determined from the linear plot in Figure 5b with $k_{app} = k_0[PhI]$ to give $k_0 = 1.7 \times 10^{-2}$ mol^{-1} dm^3 s^{-1}.

When starting from {[Pd^0(dba)$_2$] + 1 OxaPN}, the reaction order in PhI is one at low PhI concentration (Figure 5c), but a

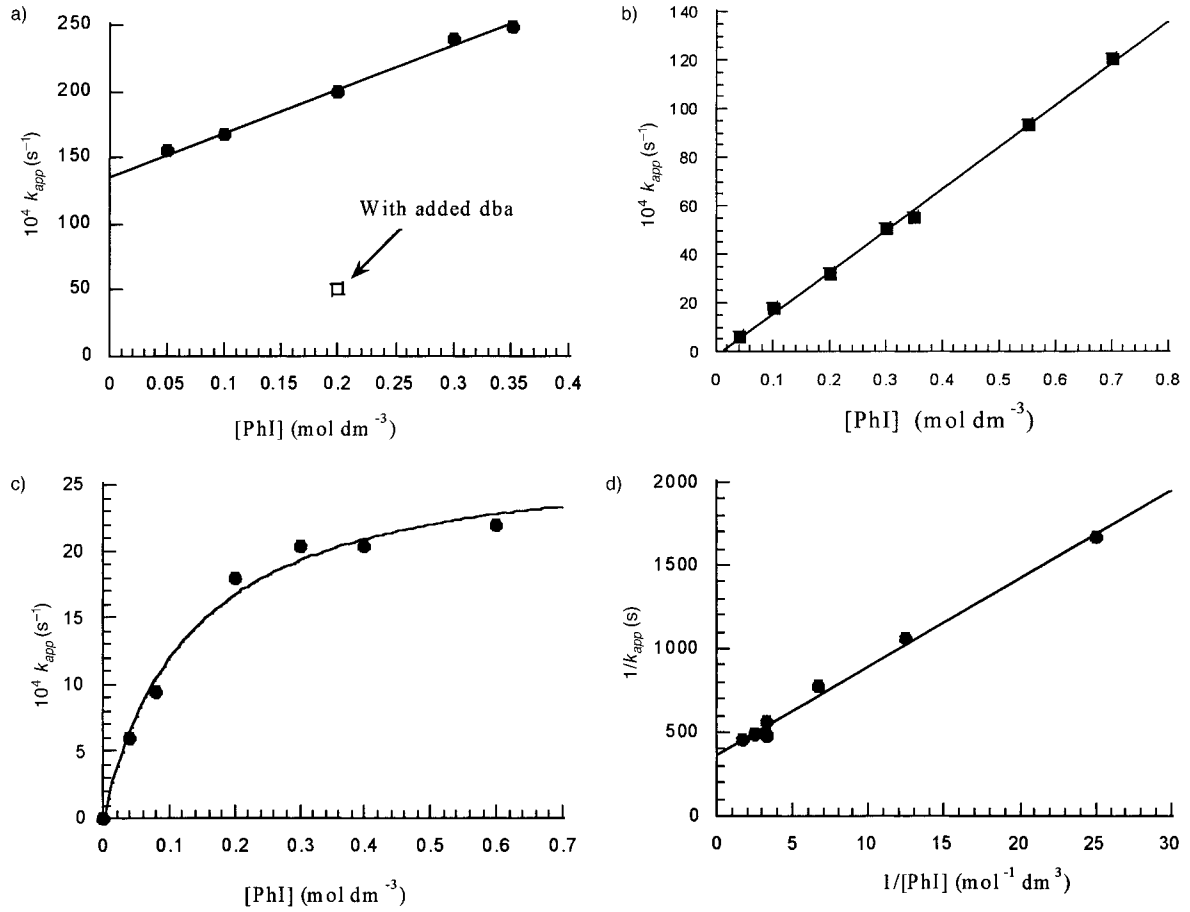

Figure 5. Oxidative addition of PhI to the palladium(0) complex generated in situ from a {[Pd(dba)$_2$] + 1P–N} mixture in THF at 40 °C. Variation of k_{app} (see text) as a function of PhI concentration: a) PhPN (●), PhPN in the presence of added dba (10 mmol dm^{-3})(□); b) FcPN; c) OxaPN; d) plot of $1/k_{app}$ versus 1/[PhI] for OxaPN.

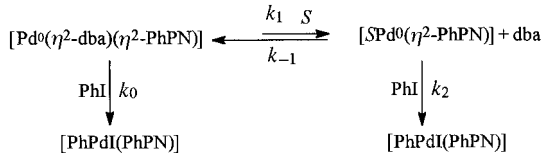

Scheme 7. Reaction of [Pd^0(dba)(PhPN)] with PhI.

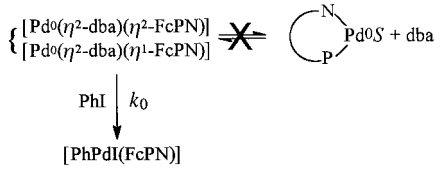

Scheme 8. Reaction of [Pd^0(dba)(FcPN)] with PhI.

saturation effect was observed at high PhI concentrations ([PhI] $\geq$ 0.3 mol dm^{-3}). The rate of the oxidative addition rate was not sensitive to variation of the dba concentration when [PhI] is sufficiently small (< 0.1 mol dm^{-3}) to correspond to the linear portion of the variations of k_{app} versus PhI concentration. This establishes that [SPd^0(OxaPN)] is not the reactive complex, so that the whole reaction proceeds through [Pd^0(dba)(OxaPN)] complexes as observed above for the FcPN ligand (Scheme 9).

At high PhI concentrations, the saturation effect shows that the kinetics are no longer controlled by the oxidative addition step but by an earlier reaction which is independent of [PhI] and which provides the reactive palladium(0) complex. Since three different [Pd^0(η^2-dba)(OxaPN)] complexes were characterized by ^{31}P NMR spectroscopy (Scheme 6), we are inclined to conclude that the reactive palladium(0) complex is the 14-electron complex [Pd^0(η^2-dba)(η^1-OxaPN)] which is slowly released from the 16-electron complexes [Pd^0(η^2-dba)(η^2-OxaPN)] by cleavage of the Pd–N bond (Scheme 9).

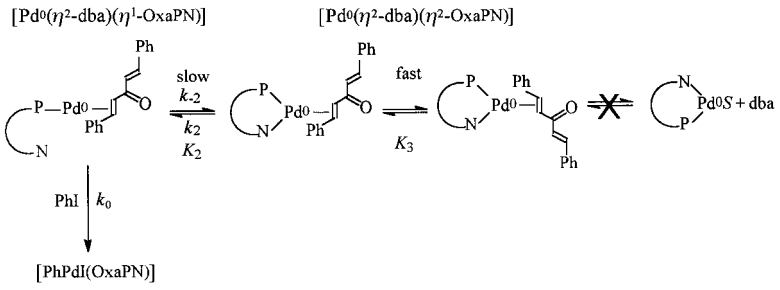

Scheme 9. Equilibria involved in the reactions of [Pd^0(dba)(OxaPN)].

0947-6539/00/0608-1480 $ 17.50+.50/0 *Chem. Eur. J.* **2000**, *6*, No. 8

Equation 10 may be derived from Scheme 9. This formula is supported by the linear plot of $1/k_{app}$ versus 1/[PhI] (Figure 5d). The values of k_2 and $k_2k_0/k_{-2} = K_2k_0$ are then determined from the intercept and the slope, respectively. A value of $K_2 = 0.25$ is available from the ratio of the ^{31}P NMR signals at δ_1 and δ_2 (Table 2), so that all the key rate constants have been determined as $k_2 = 2.8 \times 10^{-3}\ s^{-1}$, $k_{-2} = 1.1 \times 10^{-2}\ s^{-1}$ and $k_0 = 7.6 \times 10^{-2}\ mol^{-1}\,dm^3\,s^{-1}$.

$$k_{app} = \frac{k_2k_0[PhI]}{k_{-2} + k_0[PhI]} \quad \text{so that} \quad \frac{1}{k_{app}} = \frac{k_{-2}}{k_2k_0[PhI]} + \frac{1}{k_2} \qquad (10)$$

As seen above, the exchange between [Pd^0(η^2-dba)(η^2-OxaPN)] complexes was found to be fast at 40 °C ($> 10^4\ s^{-1}$). From the value of $k_2 = 2.8 \times 10^{-3}\ s^{-1}$, it is proved that [$Pd^0$($\eta^2$-dba)($\eta^1$-OxaPN)] is involved in a much slower equilibrium with [Pd^0(η^2-dba)(η^2-OxaPN)] complexes than their intrinsic equilibrium, as observed in NMR spectroscopy (see above).

The following order of reactivity has been observed (Table 3): {[Pd(dba)$_2$] + 1 PhPN} > {[Pd(dba)$_2$] + 1 FcPN} > {[Pd(dba)$_2$] + 1 OxaPN}. The reactivity of palladium(0) complexes generated from [Pd^0(dba)$_2$] and P–N ligands has been compared with that of bidentate phosphane ligands already reported (Table 3).[4] Systems involving [*S*Pd^0(P–P)] or [*S*Pd^0(P–N)] as the true reactive species in oxidative addition are found to be more reactive (diop, PhPN, dppf, except for binap) than those which involve [Pd^0(dba)(P–N)] complexes (FcPN, OxaPN) as the true reacting center. This is not surprising since [*S*Pd^0(P–P)] or [*S*Pd^0(P–N)] are more electron rich than the corresponding [Pd^0(dba)(P–P)] or [Pd^0(dba)(P–N)] complexes, so that their enhanced reactivity compensates largely for their endergonic formation from the major species present in solution.

Table 3. Comparative reactivity of Pd^0 complexes in the oxidative addition to PhI (0.2 mol dm^{-3}) as a function of the ligand associated with [Pd^0(dba)$_2$] in THF at 40 °C.

Entry	[Pd^0] = 2 mmol dm^{-3}	$t_{1/2}$ [s]
1	[Pd(dba)$_2$] + 1 diop[4]	34
2	[Pd(dba)$_2$] + 1 PhPN	50
3	[Pd(dba)$_2$] + 1 dppf [4]	110
4	[Pd(dba)$_2$] + 1 FcPN[a]	312
5	[Pd(dba)$_2$] + 1 OxaPN[a]	555
6	[Pd(dba)$_2$] + 1 binap[4]	16300

[a] When [PhI] = 0.04 mol dm^{-3}, $t_{1/2}$ was respectively 1060 s for FcPN and 1200 s for OxaPN.

For OxaPN, the actual oxidative addition step involves [Pd^0(dba)(η^1-OxaPN)] with a pseudo-first-order rate constant k_0[PhI] and is in competition with the complexation reaction that yields [Pd^0(η^2-dba)(η^2-OxaPN)] and whose rate constant is k_{-2} (Scheme 9). On the other hand, [Pd^0(η^2-dba)(η^1-OxaPN)] is constantly reformed by decoordination of [Pd^0(η^2-dba)(η^2-OxPN)] with a rate constant k_2. A saturating effect is observed when $k_{-2} \ll k_0$[PhI] and corresponds to kinetic control by the formation of [Pd^0(η^2-dba)(η^1-OxaPN)] from [Pd^0(η^2-dba)(η^2-OxaPN)]. In this situation, the rate of the overall oxidative addition is then controlled by k_2 and does not depend on the PhI concentration (Figure 5c). When considering FcPN, $k_{-2} \gg k_0$[PhI], so that a dynamic equilibrium occurs between [Pd^0(η^2-dba)(η^2-FcPN)] and [Pd^0(η^2-dba)(η^1-FcPN)]. The oxidation step is then rate-determining and the overall reaction remains apparently first order in PhI (Figure 5b). Both [Pd^0(η^2-dba)(η^2-FcPN)] and [Pd^0(η^2-dba)(η^2-OxaPN)] are six-membered rings and are thus subject to similar geometric constraints, although the bond lengths slightly differ in both complexes. Electronic effects also appear to be more important. Indeed, the NMe_2 amino group in FcPN has more σ-donor and less π-acceptor character than the oxazoline group of OxaPN, which favors a weaker coordination of the Pd^0 center by NMe_2 in [Pd^0(dba)(η^2-FcPN)] than by the oxazoline in [Pd^0(dba)(η^2-OxaPN)]. Consequently, k_2 for OxaPN is less than k_2 for FcPN. One has also to consider the intrinsic reactivity of [Pd^0(η^2-dba)-(η^1-P–N)] (k_0) defined by the basicity of the ligand as well as by its bulkiness. Once the Pd–N bond is cleaved, the P–N ligands behave as monophosphane ligands with FcPN having greater electron-donor properties than OxaPN. All these arguments would explain why {[Pd(dba)$_2$] + 1 FcPN} is slightly more reactive than {[Pd(dba)$_2$] + 1 OxaPN} (Table 3).

Conclusion

For all the P–N ligands considered in this study, [Pd^0(dba)(P–N)] is the major complex formed in solution from [Pd^0(dba)$_2$] + 1 P–N. The following isomers in equilibrium are generated: two 16-electron complexes [Pd^0(η^2-dba)(η^2-P–N)] differing by a rotation of dba around the palladium(0) center, and one 14-electron complex [Pd^0(η^2-dba)(η^1-P–N)] as observed for OxaPN and FcPN.

The behavior of PhPN is similar to that which we reported previously for bidentate bis-phosphane ligands in the sense that both [Pd^0(dba)(PhPN)] and [*S*Pd^0(PhPN)] react with PhI, [*S*Pd^0(PhPN)] being nevertheless more reactive than [Pd^0(dba)(PhPN)] because it is more electron rich. In the presence of extra PhPN ligand, [Pd^0(η^2-dba)(η^1-PhPN)$_2$] and [Pd^0(η^1-PhPN)$_3$] are formed in which PhPN behaves as a monodentate phosphane ligand, so that the situation becomes formally identical to that which we have reported for monodentate phosphanes.

With FcPN and OxaPN ligands, only [Pd^0(dba)(FcPN)] and [Pd^0(dba)(OxaPN)] are formed whatever the excess of ligand, which establishes that dba has a higher affinity for [Pd^0(P–N)] than the P–N ligand. Moreover, [*S*Pd^0(FcPN)] and [*S*Pd^0(OxaPN)] are not involved at all in the oxidative addition. The reactive palladium(0) complexes remain ligated by dba. [Pd^0(η^2-dba)(η^2-FcPN)] and [Pd^0(η^2-dba)(η^2-OxaPN)] are found to react with PhI via a 14-electron complex as established for [Pd^0(η^2-dba)(η^1-OxaPN)].

Once more, the dba ligand is found to play a crucial role in the kinetics of the oxidative addition of PhI to the palladium(0) complexes generated in situ from {[Pd^0(dba)$_2$] + 1 P–N} mixtures. It may control the concentration of the dba-free, most reactive complex (such as with PhPN) or in fact be on the reactive complex (for FcPN and OxaPN).

Experimental Section

^{31}P NMR spectra were recorded in THF on a Bruker spectrometer (162 MHz) with H_3PO_4 as an external reference. UV spectra were recorded on a DU7400 Beckman spectrophotometer. Cyclic voltammetry was performed with a home-made potentiostat and a wave form generator Tacussel GSTP4. The cyclic voltammograms were recorded on a Nicolet oscilloscope. All experiments were performed under argon. THF (Janssen) was distilled from sodium/benzophenone. The solvent was transferred to the cells according to standard Schlenk procedures. Phenyl iodide (Janssen) was filtered on neutral alumina and stored under argon. The syntheses of $[Pd(dba)_2]$,[21] PhPN,[13] and FcPN,[11] are reported in the literature. OxaPN was synthesized according to a published procedure. [12]

Characterization of OxaPN: Yield: 63%; white crystals, m.p. 96°C; ^1H NMR (200 MHz, $CDCl_3$): $\delta = 7.9-6.7$ (m, 14H; aromatic H of PPh_2), 3.74 (s, 2H; CH_2), 1.04 (s, 6H, CH_3); ^{13}C NMR (63 MHz, $CDCl_3$): $\delta = 163$, 139.5–127.9 (Ar), 78.8, 67.5, 27.9; ^{31}P NMR (163 MHz, $CDCl_3$): $\delta = -4.4$; MS (CI^+, NH_3): m/z: 360 ($[MH]^+$); $C_{23}H_{22}NOP$: calcd C 76.85, N 3.90, H 6.17; found C 76.82, N 3.95, H 6.17.

Electrochemical set-up for voltammetry: Electrochemical experiments were carried out in a three-electrode cell connected to a Schlenk line. The cell was equipped with a double envelope to maintain a constant temperature (Lauda RC20 thermostat). The working electrode consisted of a gold disk of 0.5 mm diameter. The counter electrode was a platinum wire of about 1 cm^2 apparent surface area. The reference was a saturated calomel electrode separated from the solution by a bridge filled with a solution of $n-Bu_4NBF_4$ (0.3 mol dm^{-3}) in THF (3 mL). THF (15 mL) containing the same concentration of supporting electrolyte was poured into the cell. Addition of $[Pd(dba)_2]$ (17 mg, 0.03 mmol) was followed by a suitable amount of the P–N ligand. Cyclic voltammetry was performed at a scan rate of 0.5 V s^{-1}. The kinetic measurements were performed with a rotating gold disk electrode (i.d. = 2 mm, Tacussel EDI 65109) with an angular velocity of 105 rad s^{-1} (Tacussel controvit). The potential of the rotating disk electrode was set on the oxidation plateau wave of the palladium(0) complex (wave O_1). An appropriate amount of phenyl iodide was added and the decay of the oxidation current was then monitored as a function of time.

Acknowledgements

This work has been supported in part by the Centre National de la Recherche Scientifique (CNRS, UMR 8640 "PASTEUR") and the Ministère de l'Education Nationale, de la Recherche et de la Technologie (Ecole Normale Supérieure).

[1] For a review see: C. Amatore, A. Jutand, *Coord. Chem. Rev.* **1998**, *178–180*, 511–528.
[2] C. Amatore, A. Jutand, F. Khalil, M. A. M'Barki, L. Mottier, *Organometallics* **1993**, *12*, 3168–3178.
[3] Except for the DIMFP ligand (DIMFP = tris-3,5-dimethyl-2 furylphosphane) for which $[Pd^0(DIMFP)_2]$ is the only complex formed whatever the value of *n*. C. Amatore, A. Jutand, D. Kaufmann, M. Nouroozian, unpublished results, **1998**.
[4] C. Amatore, G. Broeker, A. Jutand, F. Khalil, *J. Am. Chem. Soc.* **1997**, *119*, 5176–5185.
[5] a) T. Hayashi, M. Konishi, M. Fukushima, T. Mise, M. Kagotani, M. Tajika, M. Kumada, *J. Am. Chem. Soc.* **1982**, *104*, 180–186; b) T. Hayashi, M. Kumada, *Acc. Chem. Res.* **1982**, *15*, 395–401; c) T. Hayashi, M. Konishi, M. Fukushima, T. Kanehira, T. Hioki, M. Kumada, *J. Org. Chem.* **1983**, *48*, 2195–2202.
[6] a) U. Leutenegger, G. Umbricht, C. Fahrni, P. von Matt, A. Pfaltz, *Tetrahedron* **1992**, *48*, 2143–2156; b) P. von Matt, A. Pfaltz, *Angew. Chem.* **1993**, *105*, 614–615; *Angew. Chem. Int. Ed. Engl.* **1993**, *32*, 566–568.
[7] a) C. G. Frost, J. Howarth, J. M. J. Williams, *Tetrahedron: Asymmetry* **1992**, *33*, 1089–1121; b) C. G. Frost, J. M. J. Williams, *Tetrahedron Lett.* **1993**, *34*, 2015–2018; c) G. J. Dawson, C. G. Frost, J. M. J. Williams, S. J. Coote, *Tetrahedron Lett.* **1993**, *34*, 7793–7796.
[8] J. Sprinz, G. Helmchen, *Tetrahedron Lett.* **1993**, *34*, 3149–3150.
[9] a) O. Loiseleur, P. Meier, A. Pfaltz, *Angew. Chem.* **1996**, *108*, 218–220; *Angew. Chem. Int. Ed. Engl.* **1996**, *35*, 200–202. b) O. Loiseleur, M. Hayashi, N. Schemees, A. Pfaltz, *Synthesis* **1997**, 1338–1345.
[10] a) U. Burckhardt, V. Gramlich, P. Hofmann, R. Nesper, P. S. Pregosin, R. Salzmann, A. Togni, *Organometallics* **1996**, *15*, 3496–3503; b) P. E. Blöchl, A. Togni, *Organometallics* **1996**, *15*, 4125–4132; c) A. Togni, U. Burckhardt, V. Gramlich, P. S. Pregosin, R. Salzmann, *J. Am. Chem. Soc.* **1996**, *118*, 1031–1037.
[11] T. Hayashi, T. Mise, M. Fukushima, M. Kagotani, N. Nagashima, Y. Hamada, A. Matsumoto, S. Kawakami, M. Konishi, K. Yamamoto, M. Kumada, *Bull. Chem. Soc. Jpn.* **1980**, *53*, 1138–1151.
[12] J. V. Allen, G. J. Dawson, C. G. Frost, J. M. J. Williams, *Tetrahedron* **1994**, *50*, 799–808.
[13] L. Horner, G. Simons, *Phosphorus Sulfur* **1983**, *15*, 165–176.
[14] C. Amatore, A. Jutand, G. Meyer, *Inorg. Chim. Acta* **1998**, *273*, 76–84.
[15] Two other palladium(0) complexes might be formed in which the bulky CO–CH=CH–Ph group of the C=C bond of dba would be directed towards either the P atom or the N atom instead of the Ph group as shown in Scheme 4. Because of steric hindrance, we favor the structures presented in Scheme 4.
[16] a) R. Fernandez-Galan, F. A. Jalon, B. R. Manzano, J. R. de la Fuente, M. Vrahami, B. Jedlicka, W. Weissensteiner, G. Jogl, *Organometallics* **1997**, *16*, 3758–3768; b) F. Gomez-de la Torre, F. A. Jalon, A. Lopez-Agenjo, B. R. Manzano, A. Rodriguez, T. Sturm, W. Weissensteiner, M. Martinez-Ripoll, *Organometallics* **1998**, *17*, 4634–4644; c) K. Selvakumar, M. Valentini, M. Wörle, P. S. Pregosin, A. Albinati, *Organometallics* **1999**, *18*, 1207–1215.
[17] According to the simplified model reported in a) M. Takeda, E. Stejskal, *J. Am. Chem. Soc.* **1960**, *82*, 25–29; b) J. Sandström, *Dynamic NMR Spectroscopy*, Academic Press, New York, **1982**.
[18] R. van Asselt, C. J. Elsevier, W. J. J. Smeets, A. L. Spek, *Inorg. Chem.* **1994**, *33*, 1521–1531.
[19] A mixture of {$[Pd(dba)_2]$ + $2Ph_2P-CH_2-CH_2-NMe_2$ (EtPN)} gave rise to a similar complex $[Pd^0(\eta^2\text{-dba})(\eta^1\text{-EtPN})_2]$ with ^{31}P NMR signals at $\delta_3 = 13.97$ (d) and $\delta_4 = 14.91$ (d) with a J_{PP} coupling constant of 10 Hz.
[20] The reaction of $[SPd^0(dba)(PhPN)]$ with PhI may proceed via the 14-electron complex $[Pd^0(dba)(\eta^1\text{-PhPN})]$ although this latter complex has not been detected in ^{31}P NMR experiments because it is present in too low a concentration and/or is involved in a fast equilibrium with $[Pd^0(dba)(\eta^2\text{-PhPN})]$ complexes. These two pathways cannot be distinguished by kinetic investigation.
[21] a) Y. Takahashi, T. Ito, S. Sakai, Y. Ishii, *J. Chem. Soc. Chem. Commun.* **1970**, 1065–1066; b) M. M. F. Rettig, P. M. Maitlis, *Inorg. Synth.* **1977**, *17*, 134.

Received: August 9, 1999 [F1965]

  0947-6539/00/0608-1482 $ 17.50+.50/0